Fractional decay of quantum dots in real photonic crystals

Philip Kristensen,[1,*] A. Femius Koenderink,[2] Peter Lodahl,[1] Bjarne Tromborg,[1] and Jesper Mørk[1]

[1]*DTU Fotonik, Technical University of Denmark, Ørsteds Plads Building 343, 2800 Lyngby, Denmark*
[2]*FOM Institute for Atomic and Molecular Physics, Kruislaan 407, 1098 SJ Amsterdam, The Netherlands*
**Corresponding author: ptk@com.dtu.dk*

Received May 8, 2008; accepted June 1, 2008;
posted June 12, 2008 (Doc. ID 95972); published July 7, 2008

We show that fractional decay may be observable in experiments using quantum dots and photonic crystals with parameters that are currently achievable. We focus on the case of inverse opal photonic crystals and locate the position in the crystal where the effect is most pronounced. Furthermore, we quantify the influence of absorptive loss and show that it is a limiting but not prohibitive effect. © 2008 Optical Society of America

OCIS codes: 270.1670, 270.5580.

Spontaneous emission is a resonant process in which an emitter interacts with modes of the electromagnetic field spectrally close to the electronic transition frequency. Moving the emitter to another medium or location at which the field strength of the electromagnetic vacuum modes differ will lead to changes in the spontaneous emission. In most cases the light–matter coupling is weak, and the emitter decays exponentially in time with different decay rates at different locations. This is the weak-coupling Purcell regime.

In certain cases the coherent coupling of the emitter to a highly structured electromagnetic vacuum leads to nonexponential decays. In particular, a regime of so-called fractional decay has been pointed out [1,2]. In this regime, the emitter coherently interacts with modes of low group velocity in such a way that it never fully decays but rather remains in a superposition of the excited state and the ground state. This may happen in media with rapid variations in the spectral and spatial distribution of electromagnetic modes, as described by the local optical density of states (LDOS) [3]. Photonic crystals offer the ability to manipulate the LDOS and change it as compared to the case of a homogeneous medium. The Purcell effect has been shown experimentally for a variety of emitters, e.g, quantum dots (QDs) in inverse opal photonic crystals [4], but there has been to date no demonstration of fractional decay, to the best of our knowledge.

In this Letter we intoduce a practical measure of the degree of fractional decay and use it to investigate decay dynamics of QDs near the band edge of a photonic crystal. For calculations of decay dynamics we follow the approach of Vats *et al.* [5]. Contrary to the general treatment in [5], we focus in this Letter on the possible realization of fractional decay using specific and realistic structures. In particular the investigations are based on the actual LDOS of a three-dimensional photonic crystal obtained from plane-wave calculations and extended to include effects of absorptive losses, see Fig. 1. Absorption is shown to be a limiting factor, and we present quantitative results showing the degreee of fractional decay achievable for available QDs and practically relevant material loss.

The QD is modeled as an initially excited two-level system with transition frequency ω_{eg}, and we write the general state of the coupled electron–photon system as $|\Psi\rangle = c_e(t)|e,0\rangle + \Sigma_\mu c_{g,\mu}(t)|g,\mu\rangle$, where $|e,0\rangle$ denotes the electron in the excited state and no photons and $|g,\mu\rangle$ denotes the electron in the ground state and one photon in mode μ. The time evolution is governed by the Schrödinger equation, $i\hbar|\dot{\Psi}\rangle = \hat{H}|\Psi\rangle$, with the Hamiltonian $\hat{H}$ in the dipole and rotating-wave approximation. Using a Laplace transform [5] the equations of motion are solved in the frequency domain to yield

$$\tilde{c}_e(\mathbf{r},\tilde{\omega}) = \frac{1}{\beta G(\mathbf{r},\tilde{\omega}) - i(\tilde{\omega}-1)} = \frac{a_{-1}}{\tilde{\omega}-\tilde{\omega}_0} + \tilde{c}'(\tilde{\omega}), \quad (1)$$

where $\mathbf{r}$ is the QD position and $\tilde{\omega} = \omega/\omega_{eg}$ is the scaled frequency. We have split the spectrum into a pole

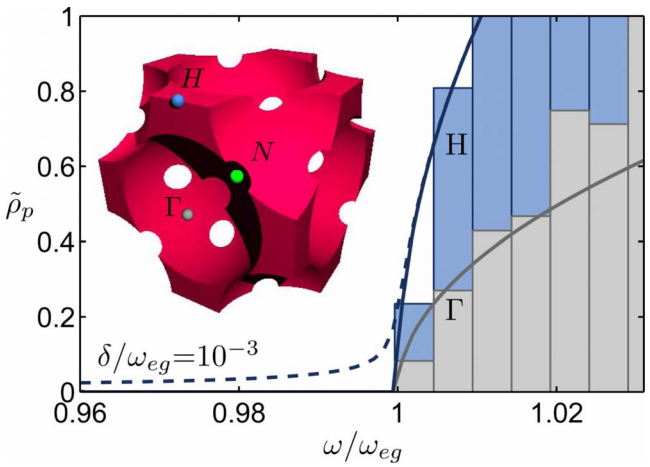

Fig. 1. (Color online) Projected LDOS of a closed packed Si inverse opal close to the band edge at the H and Γ points as indicated. Solid curves are analytical approximations to the plane-wave calculations (histograms), and the dashed curve shows the influence of loss. Inset shows the unit cell of an inverse opal and high symmetry points.

0146-9592/08/141557-3/$15.00

term with residual a_{-1}, pole position $\tilde{\omega}_0$, and a rest term. The dimensionless parameter $\beta=\Gamma_0/(2\pi\omega_{eg})$ is the vacuum decay rate Γ_0, scaled by the transition frequency, and is given as $\beta=q^2p^2/(6\hbar m^2\pi^2\epsilon_0 c^3)$, where q, p, $\hbar$, m, ϵ_0, and c denote the electron charge, the momentum matrix element, the reduced Planck constant, the electron mass, the free-space permittivity, and the vacuum speed of light, respectively. Experimental values range from $\beta\approx10^{-8}$ for InAs QDs [6] to $\beta\approx6\times10^{-8}$ for PbSe QDs [7], with so-called interface defect QDs possibly reaching values of $\beta\approx10^{-6}$ [8]. The function $G(\mathbf{r},\tilde{\omega})$ is given for frequencies above the integration path in the complex plane as

$$G(\mathbf{r},\tilde{\omega})=i\tilde{\omega}\int_0^{\tilde{\omega}_C}\frac{\tilde{\rho}_p(\mathbf{r},x)}{x^2(\tilde{\omega}-x)}\mathrm{d}x, \tag{2}$$

in which $\tilde{\rho}_p(\mathbf{r},\tilde{\omega})=\rho_p(\mathbf{r},\omega)/\rho_0(\omega_{eg})$ is the ratio of the LDOS to the vacuum LDOS at the emitter frequency. The decay is a resonant process and is governed by the LDOS in a narrow frequency interval around $\tilde{\omega}=1$. The remaining LDOS, however, does contribute an overall Lamb shift of the spectrum. To model this effect we include an integration using $\rho_p=\rho_0$ for $\tilde{\omega}<0.95$ and $1.01<\tilde{\omega}$. A cutoff is chosen at $\tilde{\omega}_C=10^5$, corresponding to the Compton frequency [5]. For $0.95<\tilde{\omega}<1.01$ the integral is carried out using the accurate LDOS $\rho_p=\rho_{BE}$, as calculated below.

The projected LDOS is defined as

$$\rho_p(\mathbf{r},\omega)=\sum_\mu|\mathbf{e}_p\cdot\mathbf{E}_\mu(\mathbf{r})|^2\delta(\omega-\omega_\mu), \tag{3}$$

where the sum is over all modes of the electromagnetic field indexed by μ, and $\mathbf{e}_p$ is the orientation of the emitter. The functions $\mathbf{E}_\mu(\mathbf{r})=\langle\mathbf{r}|\mathbf{E}_\mu\rangle$ denote the spatial and spectral distribution of the modes and are normalized as $\langle\mathbf{E}_\alpha|\epsilon_R(\mathbf{r})|\mathbf{E}_\beta\rangle_V=\delta_{\alpha,\beta}$, where ϵ_R is the relative permittivity and V is the normalization volume. In vacuum the LDOS, Eq. (3), is given as $\rho_0(\omega)=\omega^2/(3\pi^2c^3)$.

Figure 1 shows a zoom-in on the LDOS, $\tilde{\rho}_p(\tilde{\omega})$, of an Si inverse opal ($\epsilon_R=11.76$) close to the upper edge of the bandgap. The LDOS was calculated using a method similar to that of [9], corrected for the reduced symmetry of the electric field [10]. The plane-wave approach results in a discrete sampling of the LDOS, which effectively leads to incorrect results when used directly in calculations of fractional decay. Therefore we analyze analytically the LDOS in the vicinity of the upper band edge, which is defined by only the ninth band at the so-called X point [9]. Considering the contribution from just a single band, we follow [11] and rewrite the sum, Eq. (3), as

$$\rho_p(\mathbf{r},\omega)=\sum_i\frac{V}{(2\pi)^3}\int_{S(\omega)}\frac{|\mathbf{e}_p\cdot\mathbf{E}_{\mathbf{k},i}(\mathbf{r})|^2}{|\nabla\omega(\mathbf{k})|}\mathrm{d}\mathbf{k}, \tag{4}$$

in which the sum is over two different polarizations and the integration is over the dispersion surface of constant frequency ω corresponding only to the ninth band. We now expand the integrand in Eq. (4) in powers of $\mathbf{k}$ and carry out the integration. To the lowest order, the LDOS is given as $\rho_{BE}(\omega)=K_{BE}(\mathbf{r})\sqrt{\omega-\omega_{BE}}$, where ω_{BE} is the band-edge frequency and the band-edge parameter $K_{BE}(\mathbf{r})$ is related to the curvature of the dispersion surfaces and the projected electric field at the point $\mathbf{r}$. The solid curves in Fig. 1 illustrate how the square root is indeed the limiting form of the LDOS close to the band edge. Figure 2 shows values of K_{BE} along lines between symmetry points of the Wigner–Seitz cell of an Si inverse opal (hole radius per lattice constant, $R/a=0.3436$). The analytical approach allows for the use of only five $\mathbf{k}$ points in each direction for the determination of the curvature and 1243 plane waves to ensure convergence [12]. Introducing loss in the material, $\epsilon_R\rightarrow\epsilon_R+i\epsilon_I$, leads to a shift in frequency. For small losses we use first-order perturbation theory [13] to write $\omega=\omega^{(0)}-i\delta$, where $\omega^{(0)}$ is the frequency in the absence of losses and

$$\delta=\frac{\omega^{(0)}}{2}\frac{\langle\mathbf{E}_\mu|i\epsilon_I|\mathbf{E}_\mu\rangle_C}{\langle\mathbf{E}_\mu|i\epsilon_R|\mathbf{E}_\mu\rangle_V}=\frac{\omega^{(0)}\epsilon_I}{2\epsilon_R}f,$$

where subsript C denotes the volume of only the lossy material, leading to $f=\langle\mathbf{E}_\mu|\epsilon_R|\mathbf{E}_\mu\rangle_C/\langle\mathbf{E}_\mu|\epsilon_R|\mathbf{E}_\mu\rangle_V<1$. For nonzero δ we rewrite the band-edge LDOS as [11]

$$\rho_{BE}(\mathbf{r},\omega)=K_{BE}(\mathbf{r})\int_{\omega_{BE}}^{\infty}\sqrt{x-\omega_{BE}}\frac{\delta/\pi}{(\omega-x)^2+\delta^2}\mathrm{d}x,$$

which shows that the effect of absorption is to broaden the modes as well as to introduce states below the upper edge of the bandgap (dashed curve in Fig. 1).

We note that the inclusion of loss in the material compromises the expansion of the LDOS in normal modes, Eq. (3). In this case the problem can be reformulated in terms of the electromagnetic Green's function. However, in the limit of small loss, $\epsilon_I\ll\epsilon_R$, as in this work, the two formulations coincide [14], and therefore the perturbative approach is valid.

Using the above expression for $\rho_{BE}(\mathbf{r},\omega)$, the spectrum, $\tilde{c}_e(\mathbf{r},\tilde{\omega})$ is calculated from Eqs. (1) and (2). The

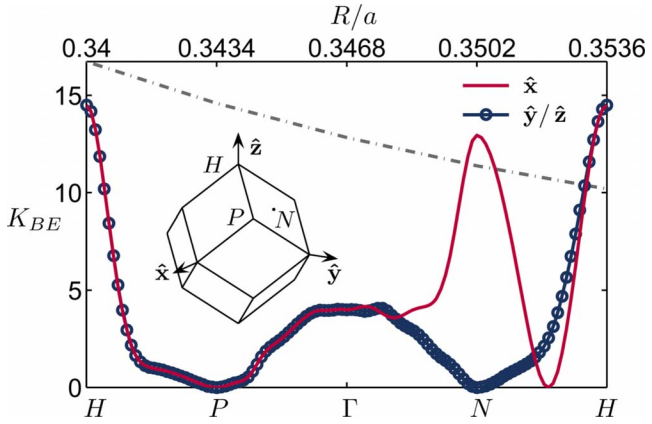

Fig. 2. (Color online) The parameter K_{BE} (in units of $\rho_0(\omega_{eg})/\omega_{eg}^{1/2}$) as a function of position in the Wigner–Seitz cell (shown in the inset) for the three principal emitter orientations. The gray dashed-dotted line shows values of K_{BE} at the H point for different R/a.

temporal evolution is subsequently obtained by transformation back to the time domain. Under this transformation, the pole term in Eq. (1) is conveniently handled analytically, resulting in a decreasing exponential part. The absolute square of the residual denotes the strength of the pole term and is equal to the value of the exponential part at $t=0$. The case of $|a_{-1}|^2=1$ results in $c'(\omega)=0$, and the spectrum consists of only a single pole term. This is characteristic of the weak coupling Purcell regime, and the decay is exponential with a decay rate $\Gamma=\Gamma_0\rho_p(\omega_{eg})/\rho_0(\omega_{eg})$. On the other hand, $|a_{-1}|^2<1$ results in a nonzero rest term and consequently a deviation from the Purcell regime, and we define $d_f=1-|a_{-1}|^2$ as a measure of the degree of fractional decay. This measure depends critically on the light–matter coupling strength βK_{BE}, relative to the absorption. The former depends on the QD as well as position in the photonic crystal, cf. Fig. 2.

For a specific example we consider now colloidal PbSe QDs, emitting at $\omega_{\mathrm{PbSe}}\approx 1.3\times10^{15}\ \mathrm{s}^{-1}$ ($\beta\approx 5.5\times10^{-8}$ [7]) and placed at the H point in a closed packed Si inverse opal ($K_{BE}\approx 10$). Figure 3 shows the resulting decay curves for different absorption. For vanishing losses, the population tends to a nonzero value at long times with $d_f=0.16$. At small finite losses a fractional effect is still visible with $d_f=0.13$ at an absorption of $\alpha=3\times10^{-5}\ \mathrm{cm}^{-1}$ ($\delta/\omega_{\mathrm{PbSe}}=10^{-10}$) and $d_f=0.04$ at $\alpha=3\times10^{-4}\ \mathrm{cm}^{-1}$ ($\delta/\omega_{\mathrm{PbSe}}=10^{-9}$). We note that absorption in Si at this frequency may be as low as $\alpha\approx10^{-7}\ \mathrm{cm}^{-1}$ ($\delta/\omega_{\mathrm{PbSe}}\approx10^{-13}$) [15]. Figure 3 therefore shows that fractional decay is observable for real QDs in dielectric photonic crystals exhibiting absorptive losses.

For a given system, the detuning of the emitter relative to the band edge defines the exact modes, and hence group velocity, of the emitted light. Therefore, the measure d_f depends also on the detuning, and we define the parameter D_f as the maximum value of d_f for optimized detuning. In Fig. 4 we show D_f as a function of βK_{BE}. The curves were obtained for each βK_{BE} by varying the detuning until a minimum was found. The figure shows that a profound degree of fractional decay is possible for a range of experimentally relevant material parameters.

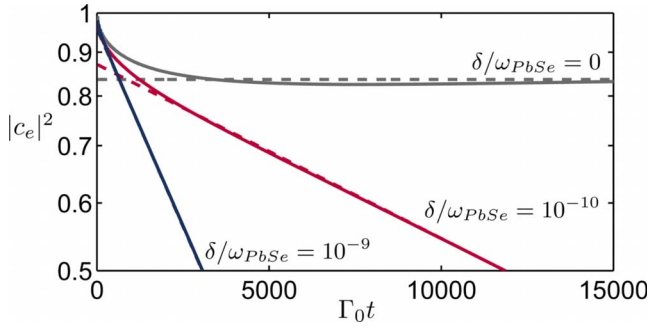

Fig. 3. (Color online) Decay from PbSe QDs at the H point in an Si inverse opal ($\beta K_{BE}=5.5\times10^{-7}$) at detuning $\omega_{BE}/\omega_{\mathrm{PbSe}}=1-8.309\times10^{-7}$ and different losses. Dashed curves show exponential parts only.

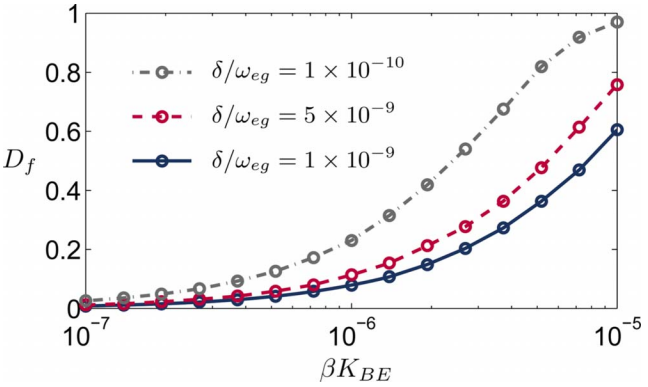

Fig. 4. (Color online) Degree of fractional decay obtainable versus light-matter coupling strength, βK_{BE}, at different absorption.

In conclusion we have used an analytic expression to the band-edge LDOS to investigate fractional decay dynamics in inverse opals. The analysis has revealed the position in the crystal that is most suitable for observation of fractional decay. Furthermore, we have extended the analysis to include absorptive losses and calculated the degree of fractional decay obtainable for given losses and light–matter coupling strengths. The analysis shows that absoption has a limiting but not prohibitive effect and that fractional decay may be possible to achieve using, e.g., PbSe QDs in Si inverse opals.

Enlightening discussions with Willem Vos and Niels Asger Mortensen are greatly appreciated.

References and Notes

1. R. F. Nabiev, P. Yeh, and J. J. Sanchez-Mondragon, Phys. Rev. A **47**, 3380 (1993).
2. S. John and T. Quang, Phys. Rev. A **50**, 1764 (1994).
3. R. Sprik, B. A. Van Tiggelen, and A. Lagendijk, Europhys. Lett. **35**, 265 (1996).
4. P. Lodahl, A. F. van Driel, I. S. Nikolaev, A. Irman, K. Overgaag, D. Vanmaekelbergh, and W. L. Vos, Nature **432**, 197 (2004).
5. N. Vats, S. John, and K. Busch, Phys. Rev. A **65**, 043808 (2002).
6. P. Yu, M. C. Beard, R. J. Ellingson, S. Ferrere, C. Curtis, J. Drexler, F. Luiszer, and A. J. Nozik, J. Phys. Chem. B **109**, 7084 (2005).
7. I. Moreels, K. Lambert, D. De Muynck, F. Vanhaecke, D. Poelman, J. C. Martins, G. Allan, and Z. Hens, Chem. Mater. **19**, 6101 (2007).
8. L. C. Andreani, G. Panzarini, and J. Gérard, Phys. Rev. B **60**, 13276 (1999).
9. S. John and K. Busch, Phys. Rev. E **58**, 3896 (1998).
10. R. Wang, X.-H. Wang, B.-Y. Gu, and G.-Z. Yang, Phys. Rev. B **67**, 155114 (2003).
11. A. A. Krokhin and P. Halevi, Phys. Rev. B **53**, 1205 (1996).
12. Values along the Γ–H route showed poor convergence and have been left out, since they are irrelevant to the conclusions in this Letter.
13. N. A. Mortensen, S. Ejsing, and S. Xiao, JEOS RP **1**, 06032 (2006).
14. T. Gruner and D.-G. Welsch, Phys. Rev. A **53**, 1818 (1996).
15. M. J. Keevers and M. A. Green, Sol. Energy Mater. Sol. Cells **41**, 195 (1996).